

Classification of motion-blurred images using Zernike and Wavelet-Fourier moments

C. Toxqui-Quitl^{*a}, A. Padilla-Vivanco^b, F. Granados-Agustín^a

^a Instituto Nacional de Astrofísica, Óptica y Electrónica; Apartado Postal 51 y 216. C. P. 72000. Tonantzintla, Puebla, México

^b División de Ingenierías, Universidad Politécnica de Tulancingo; Prolongación Guerrero No.808. C. P. 43626. Tulancingo, Hidalgo. México

ABSTRACT

In this paper, we consider the use of circular moments for invariant classification of images which have been blurred by motion. The test images used here have been acquired when the objects are vibrating at different frequencies. A comparative analysis using Zernike and Wavelet-Fourier moment sets is presented. An intensity normalization of the input images is done to homogenize them due to inhomogeneous illumination produced by the acquisition. The classification method is tested using images from objects which have intrinsically little differences between them. Experimental results show that, the proposed classification method based in Zernike and Wavelet-Fourier moments can be well addressed to grade images smeared by motion, from objects under high frequency vibrations.

Keywords: Zernike and Wavelet moments, high frequency vibration, classification of blurred images.

1. INTRODUCTION

The method of the image moments has a broad spectrum of applications such as in image reconstruction, computer vision, object classification, image analysis, invariant pattern recognition and so on. The first who proposed invariants based on geometric moments to describe an image was Hu [1]. Several years after, Teague used orthogonal polynomials to propose a new kind of moments called today, Zernike and Legendre moments [2]. Many authors have demonstrated that the moments of an image are useful features for pattern recognition and object classification [3-11]. In all these researches have been demonstrated that image moments based on different nature of polynomials can be efficiently combined in an algebraic way to define invariants to the orientation [12], scale [13], shift [14], blur [15-17], and the contrast changes [18] on the vision field of an image. Nowadays, the applications of moments has been increased and new polynomial sets have been proposed to generate invariants each time more efficient [19-22] including the n -dimensional moment invariants [23]. On the other hand, in a shape recognition system a set of numerical features are extracted from an image. These features can be invariant to different multidistorsions as the blurring caused by the motion between the camera lens and the object. Some kinds of blurring caused by vibration, constant velocity, and parabolic motion have already been analyzed using geometric moments [16]. Also, invariants based on complex moments have been proposed to recognize images blurred by the symmetrical Point spread function method [15]. Our interest of this research is to implement the circular moments of images as descriptors into a classification method of two dimensional motion-blurred images. We compare the performance of two moment sets in the classification of objects which are morphologically very similar between them. Moreover, these test objects are vibrating in the vision field. The classification of the objects is also obtained using spatial illumination variations. The kinds of moments used here are based in B -Spline Wavelet functions [3] and Zernike [2]. Our experimental results show that, the classification of the moving objects is reached using both Zernike and Wavelet moments. The kind of test objects used here are screws with millimetric and standard threads.

This paper is organized as follows: in section 2 is presented a general review of the moments of an image based in geometric and circular polynomials. This review includes a compensation method of illumination based on geometric moments to normalize the intensities in the input images. Section 3, shows the experiment and results of the

* tquitl@inaoep.mx; www.inaoep.mx

classification method using objects of two different classes. Finally in the section 4, the conclusions of work are presented.

2. IMAGE MOMENTS: A THEORETICAL REVIEW

2.1 Geometric moments

The geometric moments m_{rs} of order $r + s$ of an image $f(x, y)$ are defined as,

$$m_{rs} = \iint_{\Omega} x^r y^s f(x, y) dx dy, \quad (1)$$

where $r, s = 0, 1, 2, 3, \dots$ and Ω is the space region of pixels which is used to define the intensity function $f(x, y)$. By definition, the moment of order zero m_{00} represents the total intensity of the image and the point $(m_{10}/m_{00}, m_{01}/m_{00}) = (\bar{x}, \bar{y})$ is its intensity centroid. In the particular case of computing the area of a 8 bit binary image $f_B(x, y)$, the geometric moments can be used for this purpose by means of the relationship defined as $area = m_{00}/255$. In general, the central moments μ_{rs} computed with respect to the intensity centroid of an image are defined as,

$$\mu_{rs} = \iint_{\Omega} (x - \bar{x})^r (y - \bar{y})^s f(x, y) dx dy. \quad (2)$$

The moments of the Eq. (2) are translation invariant respect to the position of the reference system.

Particularly in the pattern recognition area, the objects of interest are frequently represented by a set of numerical features, and it is expected that; these features will be invariant to the changes in the scale, orientation, position, and illumination of objects in the vision field. All of these multidistorsions can be represented by the following transformations,

$$f_D(x', y') = g f_R(x, y), \quad (3)$$

$$\begin{bmatrix} x' \\ y' \end{bmatrix} = k \begin{bmatrix} \cos \theta & \sin \theta \\ -\sin \theta & \cos \theta \end{bmatrix} \begin{bmatrix} x \\ y \end{bmatrix} + \begin{bmatrix} x_0 \\ y_0 \end{bmatrix}, \quad (4)$$

where $f_R(x, y)$ and $f_D(x', y')$ are respectively the reference and distorted images. The number g is an intensity contrast factor, θ is an arbitrary rotation, (x_0, y_0) is the shifting in x and y directions respectively, and k is a scaling factor. The Equation (4) defines the geometric transformations suffered by the pixels of the reference image, where the coordinates of the reference and distorted images are respectively (x, y) and (x', y') . According to Mukundan [24], the geometric moments m'_{pq} of a scaled image can be expressed in terms of the moments of the reference as,

$$m'_{pq} = k^{p+q+2} m_{pq}. \quad (5)$$

In the particular case of a scale $k=1$, $m'_{pq} = m_{pq}$. Maitra [18] proposed a formula to compute the contrast factor using the central moments as follows,

$$g = k^2 \frac{\mu_{00}}{\mu'_{00}}. \quad (6)$$

This factor is sensitive to intensity changes between the images $f_R(x, y)$ and $f_D(x', y')$.

2.2 Circular Moments

Bathia and Wolf [25] pointed out that, there exist an infinite number of complete sets of polynomials which are orthogonal inside the unit circle. These polynomial sets provide rotation invariant moments of a function. A general expression for the circular moments A_{nl} of order n and repetition l for a distorted function $f_D(r, \theta)$ in polar coordinates is

$$A_{nl} = \alpha_n \cdot g \int_0^{2\pi} \int_0^k f(r/k, \theta) P_{nl}^*(r/k, \theta) r dr d\theta, \quad (7)$$

where

$$f_D(r, \theta) = g f(r/k, \theta), \quad (8)$$

and α_n is a normalization factor and the complex functions given by

$$P_{nl}(r, \theta) = \begin{cases} R_{nl}(r) \\ \psi_n(r) \end{cases} e^{il\theta}, \quad (9)$$

have radial polynomials $R_n(r)$ or $\psi_n(r)$ in r of degree n . The integers $n \geq 0$ and $l = 0, \pm 1, \pm 2, \pm 3, \dots$ are respectively the radial and the harmonic orders. If the difference $n - |l|$ is an even number for $|l| \leq n$, the radial Zernike polynomials $R_{nl}(r)$ are used in Eq. (7). Otherwise, if no restriction exists for orders n and l , then the polynomials $\psi_n(r)$ are taken into account in the same Eq. (7). It has been used the notation $\psi_n(r)$ to represent the wavelet radial functions. These functions $\psi_n(r)$ are generated by binary dilations and dyadic translations of the basic wavelet function $\psi(r)$. This set is defined as follows,

$$\psi_n(r) = 2^{p/2} \psi(2^p r - q 2^{-l}), \quad (10)$$

where the integers p and q are in terms of n , following the relationship [26],

$$n = 2^{p+l} + q + p - 2, \quad (11)$$

for $p = 0, 1, \dots, t$. and $q = 0, 1, \dots, 2^{p+1}$. If $n = 1, \dots, N-1$ then $N = 2^{t+2} + t - 2$, with t a positive integer. In particular when $N = 7$; n , p , and q are taking the values

$$n = \begin{pmatrix} 0 \\ 1 \\ 2 \\ 3 \\ 4 \\ 5 \\ 6 \\ 7 \end{pmatrix}, \quad p = \begin{pmatrix} 0 \\ 0 \\ 1 \\ 1 \\ 1 \\ 1 \\ 1 \\ 1 \end{pmatrix}, \quad q = \begin{pmatrix} 0 \\ 1 \\ 2 \\ 0 \\ 1 \\ 2 \\ 3 \\ 4 \end{pmatrix}, \quad (12)$$

where N is the number of functions to be generated. In this work will be used the cubic *B-Spline Wavelet function* $\psi(r)$ as basic wavelet [27]. It is defined by,

$$\psi(r) = \frac{4a^{m+1}}{\sqrt{2\pi(m+1)}} \sigma \cos(2\pi w(2r-1)) \exp\left(-\frac{(2r-1)^2}{2\sigma^2(n+1)}\right), \quad (13)$$

with the values $m=3$, $a=0.697066$, $w=0.409177$ and $\sigma=\sqrt{0.561145}$. The profiles for $\psi_n(r)$ with $n = 0, 1, 2, \dots, 16$, using the Eqs. (11) and (13) are shown in the Figure 1. Their respective intensity maps are shown in the Table 1. It is easy to see in the same table that, the scaling of the function is done by the integer p and the radial shifting by the parameter q . Also, the complex wavelet functions $\psi_n(r)e^{i\theta}$ can be mapped as intensity distributions in real and imaginary parts as shown in the Table 2. Commonly, the circular moments are not shift, scale and intensity changes invariant in themselves, so that; the non orthogonal Geometric [18] and Fourier Mellin moments [10] are used to normalize them. In our case the geometric moments have been implemented for this task.

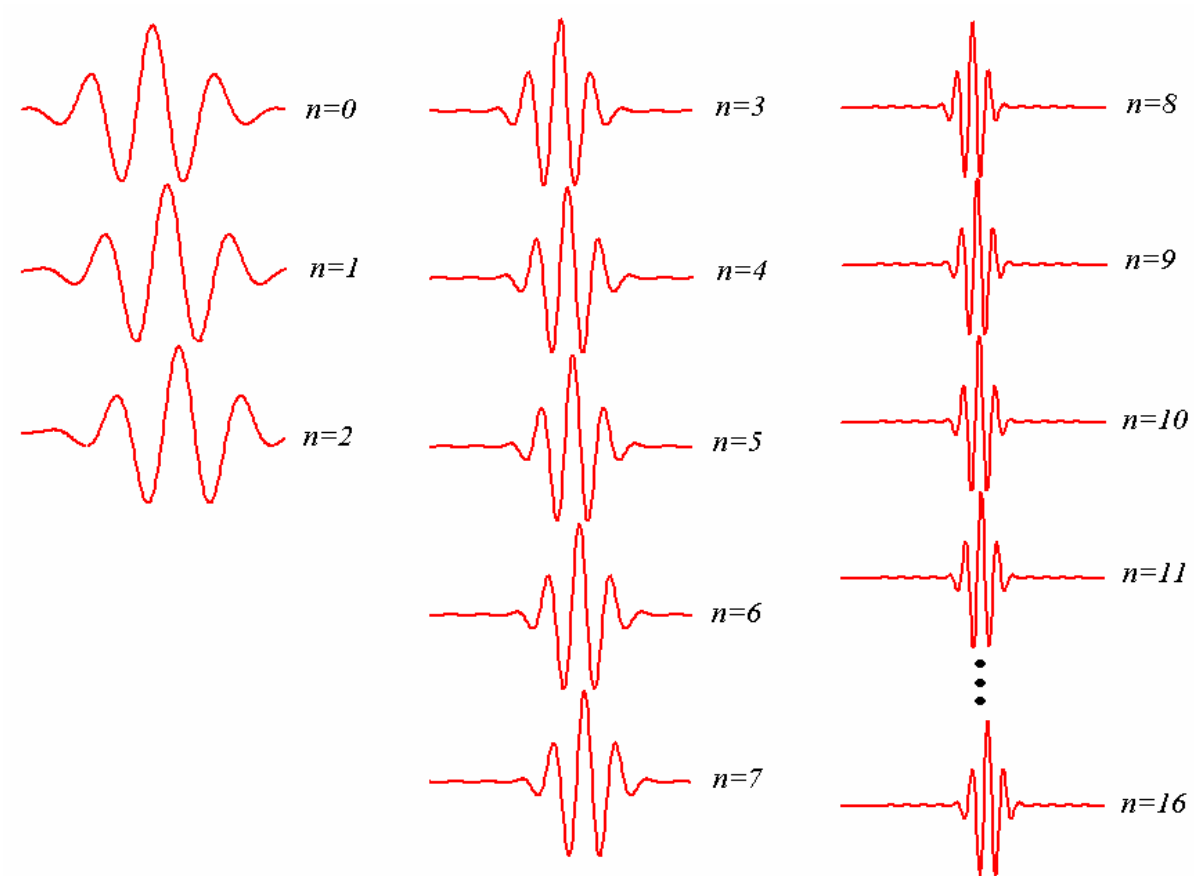


Fig. 1. Profiles of the radial B-Spline cubic Wavelet functions $\psi_n(r)$, using Eq. (11) to dilate and translate the function

Table 1. Wavelet radial intensity maps

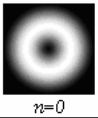
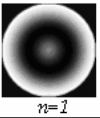
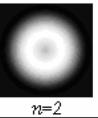
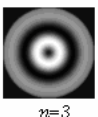
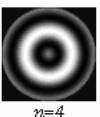
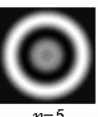
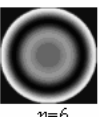




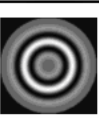










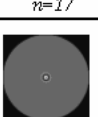
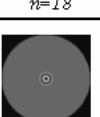






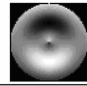
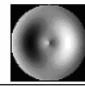
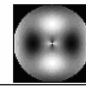
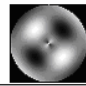
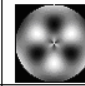
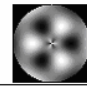
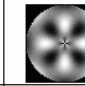
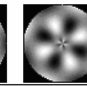
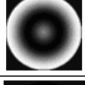
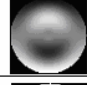
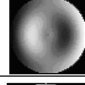
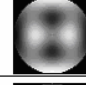
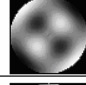
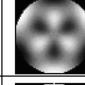
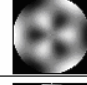

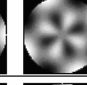
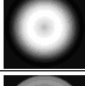
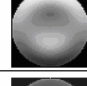
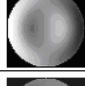
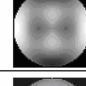
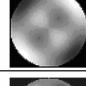
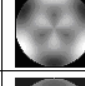
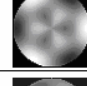
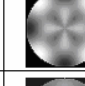
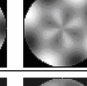
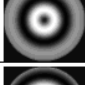
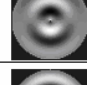
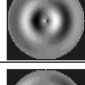
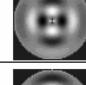
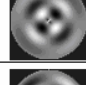

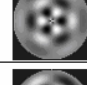
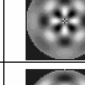
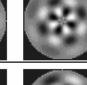
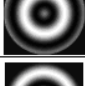
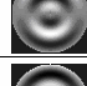
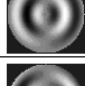





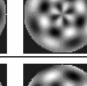
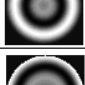
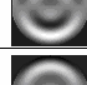
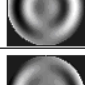
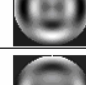
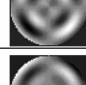

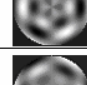
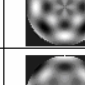
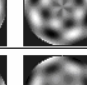




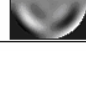
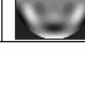

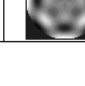

$\begin{matrix} q \\ p \end{matrix}$	0	1	2	3	4	5	...	2^{p+1}
0	 $n=0$	 $n=1$	 $n=2$					
1	 $n=3$	 $n=4$	 $n=5$	 $n=6$	 $n=7$			
2	 $n=8$	 $n=9$	 $n=10$	 $n=11$	 $n=12$	 $n=13$...	 $n=16$
3	 $n=17$	 $n=18$	 $n=19$	 $n=20$	 $n=21$	 $n=22$...	 $n=33$
4	 $n=34$	 $n=35$	 $n=36$	 $n=37$	 $n=38$	 $n=39$...	 $n=66$

Table 2. Wavelet complex intensity maps

$\begin{matrix} l \\ n \end{matrix}$	0	1	-1	2	-2	3	-3	4	-4
0									
1									
2									
3									
4									
5									
6									

2.3 Standard deviation and Mean of the moments as classification criteria

Many kinds of invariants have been proposed from several polynomial sets; as a consequence of this situation various criteria can be tested to classify objects from moments. It is however well known that, circular moments are rotation invariant and the average of a few of them from low orders can be used to define practicable measures to be implemented in practice. In this point, a simple criterion to measure the performance of the moment sets as the kind studied in the past subsection will be proposed. The objective is to obtain a classification method of objects with very little differences between them. The criterion is based in statistical metrics as the average and standard deviation of the modulus of the moments. It will be shown that, these metrics can be successfully implemented as invariant classifiers. In our experiment, the images of the objects have been multidistorsioned under hard movements as vibrations. These motions cause images blurred by the motion between the scenes and the camera lens. Specifically, the measures implemented on the modulus of A_n are given by

$$mean = \log \left[\frac{\sum_{n=0}^{\gamma-1} \sum_{l=0}^{\chi-1} |A_{nl}|}{\gamma \cdot \chi} \right], \quad (14)$$

and

$$deviation = \log \left[\frac{\sum_{n=0}^{\gamma-1} \sum_{l=0}^{\chi-1} |A_{nl}|^2}{\gamma \cdot \chi} - \left(\frac{\sum_{n=0}^{\gamma-1} \sum_{l=0}^{\chi-1} |A_{nl}|}{\gamma \cdot \chi} \right)^2 \right], \quad (15)$$

where γ and χ are respectively the maximum values computed for the radial and harmonic orders. During the classification of the objects is required to compare the number of moments μ computed in the Eq. (7), for each polynomial set. This number depends of the kind of radial polynomials used. If the $R_n(r)$ polynomials are used, thus; the number of moments is

$$\mu = \sum_{i=0}^{\gamma_z} \left\{ \left\lfloor \frac{i}{2} \right\rfloor + 1 \right\}, \quad (16)$$

where the symbol $\lfloor \beta \rfloor$ is the integer part of β . On the other hand, if the $\psi_n(r)$ is implemented the number μ is computed using the expression,

$$\mu = (\gamma_\psi + 1)^2. \quad (17)$$

The radial orders in both cases are related by

$$\gamma_z = 2\gamma_\psi, \quad (18)$$

where the γ_z and γ_ψ are the maximum values of the radial orders computed, respectively for $R_n(r)$ and $\psi_n(r)$.

3. EXPERIMENT AND RESULTS

The kind of objects used in this research correspond to mechanical parts, they are set on a mobile base to be digitized with an optical digital system. The arrangement consists of a 1/2 in. CCD B&W camera (1392×1040 px) with a video frame rate of 30 frames/s, a 35-75 mm zoom lens, an incoherent illumination system with a white light illuminator (10 to 30 W), and a monochrome frame grabber with video up to 60 MHz of pixel rate and a pixel resolution up to 2048×2048. The vibration-blurred images used here are produced by changes in the oscillation frequency of a loudspeaker bellows that is used to vibrate the input objects. The control of the oscillation frequencies is done by the union of a signal generator along with an electronic amplifier connected to the loudspeaker. The interval of frequencies reached by the bellows is $\{1, 2, 3, \dots, 9\}$ Hz. Some images of screws blurred by vibration are shown in the Figure 2, and the oscillating system is sketched in the Figure 3.











Thread	Frequency				
	1 Hz.	3 Hz.	5 Hz.	7 Hz.	9 Hz.
Millimetric					
Standard					

Figure 2. Images of screws smeared by vibration. Each frequency increases the blurring in the vertical direction of the image

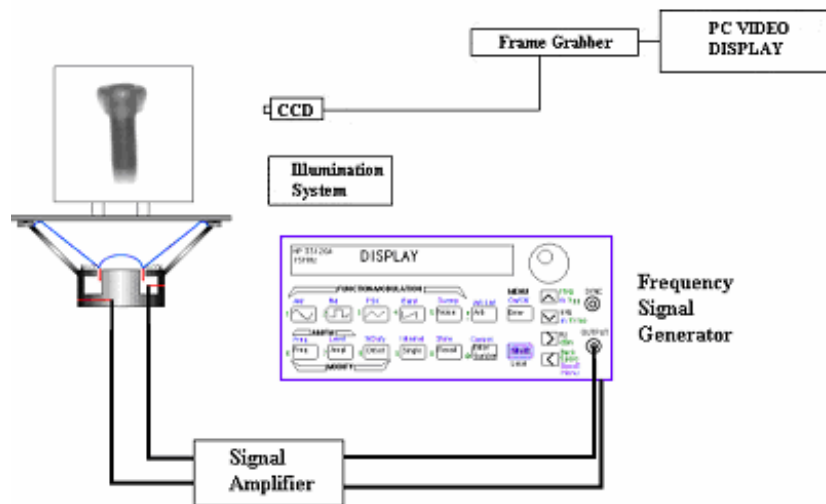


Figure 3. Sketch of a vibration system to produce blurring in the test images, it is composed by a loudspeaker bellows, an electronic signal amplifier, and a frequency generator

When the image acquisition of the objects is finished, their image moments are computed using the Eq. (7). The intensity normalization factor g obtained via the relation (6) has been taken into account in the computation of the A_{nl} . Now we are in position of using the Eqs. (14), to obtain the mean of the modulus of the moments. After computing the mean of the Zernike and Wavelet moments of the images, the obtained values are graphed as shown in the Fig. 4. As it can be seen in the graphs, there exist a distance between the values of the means for the two classes of objects studied. The classification criterion works as shown in the Figure 4, because it is evident that; in every case only the curves from the same class of screws are crossed.

4. CONCLUSIONS

We have computed circular moments on the basis sets of Zernike and Wavelet to classify motion-blurred images. An experimental setup has been implemented to acquired images blurred by vibration. The test objects have been acquired in oscillating motions at different frequencies. The classification method has been proven with test objects as screws which have very similar features between them. The object classification using circular moments is limited to a maximum frequency. In our experiment this maximum frequency is 7 Hz. The blurring in the images produced by the motion is controlled by a loudspeaker bellows. All the moment sets are averaged using the Eqs. (14), this expression is used as an invariant, it has been proposed as a classification criterion to grade images in classes. The first class corresponds to the millimetric thread and the second to the standard. The classification is reached when the values of the mean of the modulus of the moments are crossed between objects from the same class. And not works when these values from objects of different classes are mixed between them. In general the circular complex moments have been found well addressed to discriminate objects with high similarities. The experimental results shows that the proposed classification method based on Wavelet and Zernike moments have a good performance.

REFERENCES

1. M. K. Hu, "Visual pattern recognition by moment invariants," *IRE Trans. Inform. Theory* IT-8, 179-187, (1962).
2. M. R. Teague, "Image analysis via the general theory of moments," *J. Opt. Soc. Am.* 70, 920-930, (1980).
3. Dinggang Shen, Horace H. S. Ip, "Discriminative wavelet shape descriptors for recognition of 2-D patterns". *Pattern Recognition* 32, 151-165 (1999).
4. C. Kan and M.D. Srinath, "Combined features of cubic B-Spline Wavelet Moments and Zernike moments for invariant character recognition" *Proc. of the International conf. on inform Tech: (ITCC 2001)*.
5. C. Kan and M. D. Srinath, "Invariant character recognition with Zernike and orthogonal Fourier-Mellin moments," *Pattern recognition*, 35, 143-154 (2002).
6. S. O. Belkasin, "Pattern recognition with moment invariants - A comparative study and new results," *Pattern recognition*, 24, No. 12, 1117-1138 (1991).
7. R. J. Prokop and A. P. Reeves, "A survey of moment-based techniques for unoccluded object representation and recognition," *J. Graph. Models Image Process.* 54, 438-460 (1992).
8. A. Khotanzad, "Object recognition using a neural network and invariance Zernike features," *Intl. Conf. on Comput. Vision and Patt. Recognition*, 200-207, (1989).
9. T. Xia, H. Zhu, H. Shu, P. Haigron and L. Luo, "Image description with generalized pseudo-Zernike moments," *J. Opt. Soc. Am. A* 24, 50-59, (January 2007).
10. Y. L. Sheng and L. X. Shen, "Orthogonal Fourier-Mellin moments for invariant pattern recognition," *J. Opt. Soc. Am. A* 11, 1748-1757 (1994).
11. H. Ren, Z. Ping, W. Bo, W. Wu, and Y. Sheng, "Multidistorsion-invariant image recognition with radial harmonic Fourier moments" *J. Opt. Soc. Am A* 20, 631-637 (2003).
12. Flusser J. "On the independence of rotation moment invariants". *Pattern Recognition* 33 (9), 1405-1410, (2000).
13. C. Chong, P. Raveendran, and R. Mukundan, "Translation and scale invariants of the Legendre moments," *Pattern Recognition*, 37, 119-129, (2004).
14. C. Chong, P. Raveendran, and R. Mukundan, "Translation invariants of Zernike moments," *Pattern Reconition.* 36, 1765-1773, (2003).

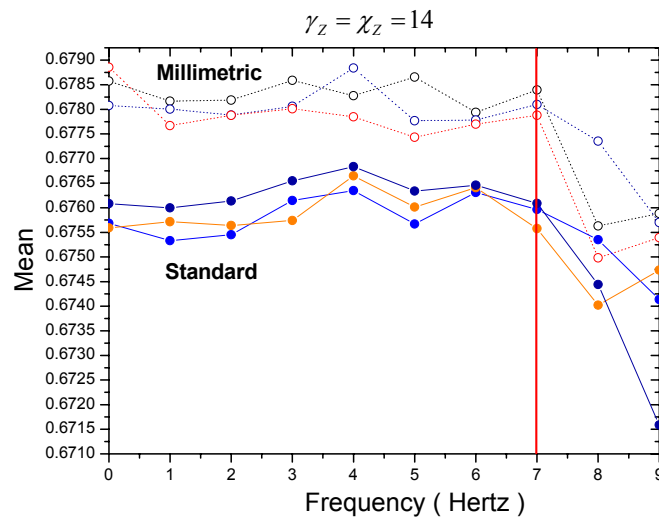
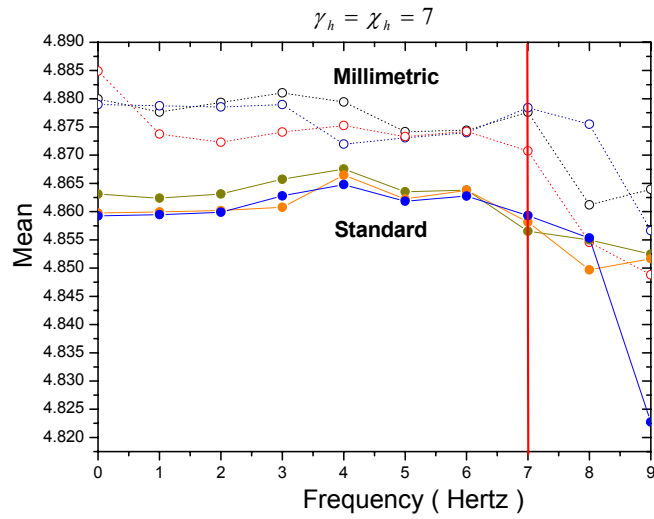


Figure 4. a) Classification of six screws in terms of their threads using the mean of a) Wavelet-Fourier, and b) Zernike moments. The curves in the above position in each graph correspond to the three millimetric screws and the curves below, belong to the three standards. The vertical lines indicate the limit frequency of classification. Both Wavelet and Zernike moments reach the classification until 7 Hz of frequency.

15. A. Stern and N. S. Kopeika, "Analytical method to calculate optical transfer function for image motion and vibrating using moments," *J. Opt. Soc. Am. A* 14, 388-396 (1997).
16. A. Stern, I. Kruchakov, E. Yoavi, and N. Kopeika, "Recognition of motion-blurred images by use of the method of moments," *Applied Optics* 41 (11), 2164-2171, (2002).
17. J. Liu, and T. Zhang, "Recognition of the blurred image by complex moment invariants," *Pattern Recognition Letters* 26, 1128-1138, (2005).
18. S. Maitra, "Moment Invariants," *Proceedings of the IEEE* 67 (4), 697-699, (1979).
19. Z. L. Ping, R. G. Wu, and Y. L. Sheng, "Image description with Chebyshev-Fourier moments," *J. Opt. Soc. Am. A* 19, 1748-1754, (2002).
20. G. Amu, S. Hasi, X. Yang, and Z. Ping, "Image analysis by Pseudo-Jacobi ($p=4$, $q=3$)-Fourier moments," *J. Opt. Soc. Am. A* 43 (10), 2093-2101, (2004).
21. R. Mukundan, "Image analysis by Tchebichef moments," *IEEE Transactions on Image Processing*, 10 (9), 1357-1364, (2001).
22. P. T. Yap, R. Paramesan, "Image analysis by Krawtchouk moments," *IEEE Transactions on Image Processing*, 12 (11), 1367-1377, (2003).
23. A. G. Mamistvalov, " n -Dimensional Moment Invariants and Conceptual Mathematical Theory of Recognition n -dimensional Solids," *IEEE Transactions on Pattern Analysis and Machine Intelligence*, 20 (8), 819-830, (1998).
24. R. Mukundan and K. R. Ramakrishnan, *Moment Functions in Image Analysis*. World Scientific, Singapore (1998).
25. A. B. Bhatia and E. Wolf, "On circular polynomials of Zernike and related orthogonal sets," *Proc. Cambridge Philos. Soc.* 50, 40-48 (1954).
26. C. Toxqui-Quitl, *Master degree Thesis*. Clasificación de objetos usando los momentos de una imagen, INAOE, Tonantzintla, Puebla, México (2006).
27. Michael Unser, Akram Aldroubi and Murray Eden, "On the Asymptotic Convergence on B - Spline wavelets to Gabor functions". *IEEE Trans. Inform. Theory* 38, 864-871 (1992).